H∞ observer for road profile estimation in an automotive semi-active suspension system using two accelerometers

Thanh-Phong Pham, Olivier Sename, Cao Tho Phan, Gia Quoc Bao Tran

H_∞ observer for road profile estimation in an automotive semi-active suspension system using two accelerometers

Thanh-Phong Pham[1], Olivier Sename[2], Cao Tho Phan[1], and Gia Quoc Bao Tran[2]

[1] The University of Danang - University of Technology and Education, Danang 550000, Vietnam,
{ptphong;pctho}@ute.udn.vn,
[2] Univ. Grenoble Alpes, CNRS, Grenoble INP$^\top$, GIPSA-lab, 38000 Grenoble, France
$^\top$Institute of Engineering
olivier.sename@ gipsa-lab.grenoble-inp.fr;
gia-quoc-bao.tran@grenoble-inp.org,

Abstract. This work presents an H_∞ observer design for road profile estimation in the automotive semi-active suspension system. The dynamics of the quarter-car augmented with a nonlinear dynamic model of the semi-active damper are written into the descriptor system with road profile as the system states. Then an H_∞ observer is developed to estimate the road profile using the onboard accelerometers as the observer's input. The objective is to minimize the effect of sensor noises on the estimation error using H_∞ framework. The estimation approach is simulated on the quarter-car model of a scaled testbench of Gipsa-lab. Simulation results show the effectiveness of the proposed method.

Keywords: H_∞ observer, road profile estimation, descriptor system

1 Introduction

In automotive applications, the road profile is considered one of the main factors influencing the vehicle system's performance. Therefore, the real-time knowledge of road input plays a vital role in the automotive suspension control system (see [16, 14, 13] and references therein). Many suspension control approaches are developed under the standard assumption of real-time access (through measurement or estimation methods) of road disturbance such as [15], [6]. In which, the profile measurements based either on profilometers presented in [9], [1] or on visual inspection in [18]. As an alternative and preventive, the estimation strategies are utilized to estimate the road profile since its direct measurement is more expensive.

Many estimation approaches are introduced to estimate the road profile using onboard sensors. The work in [17] presented an artificial neural network (ANN) based method to estimate the road excitation, using accelerometers. Besides, [20]

developed H_∞ observer considering the road profile as an unknown input to estimate the variables of the suspension system in the first step. The second step was using the above-estimated states, the unsprung mass accelerometer data, and the quarter-car model to obtain the road profile. On the other hand,[19] and [5] presented the adaptive estimation method based on Youla–Kučera (YK) parametrization for road profile estimation and classified the road roughness according to ISO standard using Fourier transform. Although the presented results are exciting, it is also worth noting that the above method required the sprung mass displacement sensor as an input.

On the other hand, using a state observer to estimate the road profile needs a differential equation for the road profile variable. However, it is not easy to model for any road profile. Some models are today used as in [19] and [7] but these are valid for a specific ISO classification only. In order to deal with this changeling, the dynamic system can be model as a descriptor system. Then we can use the robust observer for the descriptor system presented in [10, 3, 8, 4] to estimate the road profile. The method given in this work is an H_∞ observer to estimate road profile using two accelerometers of the quarter-car model. First, the dynamic system needs to represent a descriptor system to avoid using the differential equation of road profile while the nonlinearity in the damper model satisfies a Lipschitz condition. An H_∞ observer is then developed, following the parameterisation steps in [4], in which the H_∞ framework is used to minimize the effect of sensor noises on the estimation error and the nonlinearity in the dynamic model is bounded via Lipschitz condition. The main contributions of this work are as follows:

- We do not need any equation describing the road profile since the quarter-car model with a dynamical nonlinear damper model is written into a nonlinear descriptor system. The H_∞ observer for the nonlinear descriptor system is then developed to estimate the road profile, minimizing the sensor noise effect on the estimation errors.
- The proposed observer has been simulated on a scaled-vehicle test bench model, which model evaluated by the experimental tests.

The rest of this paper is as follows. Section 2 presents the dynamic model of the quarter car suspension system and the nonlinear descriptor reformulation. Section 3 develops the H_∞ observer design. In section 4, the method is analyzed in the frequency domain. Some simulation results in the time domain are presented in Section 5. Finally, section 6 gives some concluding remarks.

2 Semi-active suspension modeling and quarter-car system description

2.1 Quarter-car system description

This section presents the quarter-car model with the semi-active ER suspension system. The well-known model consists of the sprung mass (m_s), the unsprung

mass (m_{us}), the suspension components located between (m_s) and (m_{us}) and the tire which is modelled as a spring with stiffness k_t. From Newton's second law of motion, the system dynamics around the equilibrium are given as:

$$\begin{cases} m_s \ddot{z}_s & = -F_s - F_d \\ m_{us} \ddot{z}_{us} & = F_s + F_d - F_t \end{cases} \tag{1}$$

where $F_s = k_s(z_s - z_{us})$ is the spring force; $F_t = k_t(z_{us} - z_r)$ is the tire force; the damper force F_d is given as follows (see [11, 12]):

$$\begin{cases} F_d & = k_0(z_s - z_{us}) + c_0(\dot{z}_s - \dot{z}_{us}) + F_{er} \\ \dot{F}_{er} & = -\frac{1}{\tau} F_{er} + \frac{f_c}{\tau} \cdot u \cdot tanh(k_1(z_s - z_{us}) + c_1(\dot{z}_s - \dot{z}_{us})) \end{cases} \tag{2}$$

where $c_0, c_1, k_0, k_1, f_c, \tau$ are constant parameters; z_s and z_{us} are the displacements of the sprung and unsprung masses, respectively. z_r is the road displacement input.

All of the system's parameters are shown in table 1.

Table 1. Parameter values of the quarter-car model equipped with an ER damper

Parameter	Description	value	Unit
m_s	Sprung mass	2.27	kg
m_{us}	unsprung mass	0.25	kg
k_s	Spring stiffness	1396	N/m
k_t	Tire stiffness	12270	N/m
k_0	Passive damper stiffness coefficient	170.4	N/m
c_0	Viscous damping coefficient	68.83	N.s/m
k_1	Hysteresis coefficient due to displacement	218.16	N.s/m
c_1	Hysteresis coefficient due to velocity	21	N.s/m
f_c	Dynamic yield force of ER fluid	28.07	N
τ	Time constant	43	ms

2.2 Descriptor system modeling

By selecting the system states as $x = [x_1, x_2, x_3, x_4, x_5, x_6]^T = [z_s, \dot{z}_s, z_{us}, \dot{z}_{us}, F_{er}, z_r]^T \in \mathbb{R}^{n_x}$, the measured variables $y = [\ddot{z}_s, \ddot{z}_{us}]^T \in \mathbb{R}^{n_y}$ (notice that in our application $n_x = 6$ and $n_y = 2$), the system dynamics can be written in the following descriptor system form:

$$\begin{cases} E\dot{x} & = Ax + B\Phi(Ex) \cdot u \\ y & = Cx + D\omega \end{cases} \tag{3}$$

where ω is the sensor noises. The nonlinear function $\Phi(Ex) = tanh(k_1 x_1 + c_1(x_2 - x_4)) = tanh(\Gamma_e x)$ with $\Gamma_e = \begin{bmatrix} k_1, & c_1, & -k_1, & -c_1, & 0 & 0 \end{bmatrix}$. Notice that the nonlinear

function $\Phi(Ex)$ satisfies the Lipschitz condition in x

$$\|\Phi(Ex) - \Phi(E\hat{x})\| \leqslant \|\Gamma_e(x - \hat{x})\|, \forall x, \hat{x} \tag{4}$$

where

$$E = \begin{bmatrix} 1&0&0&0&0&0 \\ 0&1&0&0&0&0 \\ 0&0&1&0&0&0 \\ 0&0&0&1&0&0 \\ 0&0&0&0&1&0 \end{bmatrix}, A = \begin{bmatrix} 0 & 1 & 0 & 0 & 0 & 0 \\ -\frac{(k_s+k_0)}{m_s} & -\frac{c_0}{m_s} & \frac{(k_s+k_0)}{m_s} & \frac{c_0}{m_s} & -\frac{1}{m_s} & 0 \\ 0 & 0 & 0 & 1 & 0 & 0 \\ \frac{(k_s+k_0)}{m_{us}} & \frac{c_0}{m_{us}} & -\frac{(k_s+k_0+k_t)}{m_{us}} & -\frac{c_0}{m_{us}} & \frac{1}{m_{us}} & \frac{k_t}{m_{us}} \\ 0 & 0 & 0 & 0 & -\frac{1}{\tau} & 0 \end{bmatrix}$$

$$C = \begin{bmatrix} -\frac{(k_s+k_0)}{m_s} & -\frac{c_0}{m_s} & \frac{(k_s+k_0)}{m_s} & \frac{c_0}{m_s} & -\frac{1}{m_s} & 0 \\ \frac{(k_s+k_0)}{m_{us}} & \frac{c_0}{m_{us}} & -\frac{(k_s+k_0+k_t)}{m_{us}} & -\frac{c_0}{m_{us}} & \frac{1}{m_{us}} & \frac{k_t}{m_{us}} \end{bmatrix}, B = \begin{bmatrix} 0 \\ 0 \\ 0 \\ 0 \\ \frac{f_c}{\tau} \end{bmatrix}, D = \begin{bmatrix} 0.01 \\ 0.01 \end{bmatrix}$$

3 H_∞ Observer design

The reduced-order H_∞ observer for the quarter-car system (3) is chosen as:

$$\begin{cases} \dot{z} = Nz + Jy + H\Phi(E\hat{x}) \cdot u \\ \hat{x} = Rz + Sy \end{cases} \tag{5}$$

where $z \in \mathbb{R}^{n_x - n_y}$ is the state variable of the observer, here $z \in \mathbb{R}^4$, $\hat{x}$ is the estimated state of x. The observer matrices N, L, H, J, S appropriate dimensions have to be designed.

The dynamic error is given as follows:

$$\epsilon = z - TEx, \tag{6}$$

where the matrix T is an arbitrary matrix.

Differentiating (6) with respect to time and using (3) and (5), leads to:

$$\begin{cases} \dot{\epsilon} & = \dot{z} - TE\dot{x} \\ & = N\epsilon + (NTE - TA + JC)x + JD\omega + (H - TB) \cdot \Phi(E\hat{x})u \\ & -TB \cdot (\Phi(Ex) - \Phi(\hat{E}x))u \\ \hat{x} & = R\epsilon + (RTE + SC)x + SD\omega. \end{cases} \tag{7}$$

It is obvious that if the following decoupling conditions are satisfied:

$$NTE - TA + JC = 0 \tag{8}$$

$$H - TB = 0 \tag{9}$$

$$RTE + SC = I \tag{10}$$

the system (7) becomes

$$\begin{cases} \dot{\epsilon} &= N\epsilon - TB\Delta\Phi + JD\omega \\ e &= R\epsilon + SD\omega. \end{cases} \tag{11}$$

where $e = \hat{x} - x$ is the state estimation error and $\Delta\Phi = \Phi(Ex) - \Phi(E\hat{x}) \cdot u$.

In our application, u is the duty cycle of PWM signal. Therefore, it is worth noting that the maximum value of u is 1. Therefore, the term $\Delta\Phi$ is bounded by $0 \leq \Delta\Phi \leq \Phi(Ex) - \Phi(E\hat{x})$.

The problem of the $\mathcal{H}_\infty$ observer design reduces to determine the observer matrices N, J, H, R, S such that all conditions (8)-(10) are satisfied and the effect of measurement noise ω on the state estimation error e is minimized while $\Delta\Phi$ is bounded.

3.1 Parameterization of the observer matrices

In order to determine the observer matrices N, J, H, R, S of the proposed observer satisfying all the conditions equalities (8)-(10), the parameterisation is made by using the general solution of (8) and (10). The parameterization steps in here are similar with [4].

Firstly, from equations (8) and (10), one obtained

$$\begin{pmatrix} N & J \\ R & S \end{pmatrix} \begin{pmatrix} TE \\ C \end{pmatrix} = \begin{pmatrix} TA \\ I \end{pmatrix}. \tag{12}$$

The equation (12) is solvable if and only if

$$rank \begin{pmatrix} TE \\ C \\ TA \\ I \end{pmatrix} = rank \begin{pmatrix} TE \\ C \end{pmatrix} = n_x. \tag{13}$$

Next, let matrix $M \in \mathbb{R}^{n_x \times n_x}$ be an arbitrary matrix of full row rank such that:

$$rank \begin{pmatrix} M \\ C \end{pmatrix} = rank \begin{pmatrix} TE \\ C \end{pmatrix} = n_x. \tag{14}$$

Then there always exists a parameter matrix K such that:

$$\begin{pmatrix} TE \\ C \end{pmatrix} = \begin{pmatrix} I & -K \\ 0 & I \end{pmatrix} \begin{pmatrix} M \\ C \end{pmatrix} \Leftrightarrow TE = M - KC \tag{15}$$

$$\Rightarrow \begin{pmatrix} T & K \end{pmatrix} \begin{pmatrix} E \\ C \end{pmatrix} = M \tag{16}$$

A solution for (14) is given by

$$\begin{pmatrix} T & K \end{pmatrix} = M\Sigma^+ \tag{17}$$

where $\Sigma = \begin{pmatrix} E & C \end{pmatrix}$, Σ^+ is any general inverse of matrix Σ satisfying $\Sigma\Sigma^+\Sigma = \Sigma$. This is equivalent to:

$$T = M\Sigma^+ \begin{pmatrix} I \\ 0 \end{pmatrix}, \quad K = M\Sigma^+ \begin{pmatrix} 0 \\ I \end{pmatrix} \tag{18}$$

Besides, the solution set of (12) is given by

$$\begin{pmatrix} N & J \\ R & S \end{pmatrix} = \begin{pmatrix} TA \\ I \end{pmatrix} \begin{pmatrix} TE \\ C \end{pmatrix}^+ + \begin{pmatrix} Z_1 \\ Z_2 \end{pmatrix} \left(I - \begin{pmatrix} TE \\ C \end{pmatrix} \begin{pmatrix} TE \\ C \end{pmatrix}^+ \right). \tag{19}$$

where $\begin{pmatrix} Z_1 \\ Z_2 \end{pmatrix}$ is a free matrix of appropriate dimension. This is equivalent to:

$$N = TA\alpha_1 + Z_1\beta_1 \tag{20}$$
$$J = TA\alpha_2 + Z_1\beta_2 \tag{21}$$
$$R = \alpha_1 + Z_2\beta_1 \tag{22}$$
$$S = \alpha_2 + Z_2\beta_2 \tag{23}$$

where $\alpha_1 = \begin{pmatrix} TE \\ C \end{pmatrix}^+ \begin{pmatrix} I \\ 0 \end{pmatrix}$, $\alpha_2 = \begin{pmatrix} TE \\ C \end{pmatrix}^+ \begin{pmatrix} 0 \\ I \end{pmatrix}$, $\beta_1 = \left(I - \begin{pmatrix} TE \\ C \end{pmatrix} \begin{pmatrix} TE \\ C \end{pmatrix}^+ \right) \begin{pmatrix} I \\ 0 \end{pmatrix}$, $\beta_2 = \left(I - \begin{pmatrix} TE \\ C \end{pmatrix} \begin{pmatrix} TE \\ C \end{pmatrix}^+ \right) \begin{pmatrix} 0 \\ I \end{pmatrix}$.

Remark: If the matrices N, J, R, S, H can be chosen according to (20), (21), (22), (23) and (9), respectively, then, all conditions (8)-(10) are fulfilled.

From the results of above parameterization, for simplicity, the matrices of system (11) can be rewritten as follows:

$$\mathbb{A}_1 = N = A_{11} + Z_1A_{12} \tag{24}$$
$$\mathbb{B}_1 = JD = B_{11} + Z_1B_{12} \tag{25}$$
$$\mathbb{W}_1 = -TB \tag{26}$$
$$\mathbb{C}_1 = R = C_{11} + Z_2C_{12} \tag{27}$$
$$\mathbb{D}_1 = SD = D_{11} + Z_2D_{12} \tag{28}$$

where $A_{11} = TA\alpha_1$, $A_{12} = \beta_1$, $B_{11} = TA\alpha_2D$, $B_{12} = \beta_2D$, $C_{11} = \alpha_1$, $C_{12} = \beta_1$, $D_{11} = \alpha_2D$, $D_{12} = \beta_2D$

Notice that all the matrices A_{11}, A_{12}, B_{11}, B_{12}, $\mathbb{W}_1$, C_{11}, C_{12}, D_{11}, D_{12} are known.

3.2 $\mathcal{H}_\infty$ design

Using (24)-(28), the estimation error dynamic system (11) is rewritten as:

$$\begin{cases} \dot{\epsilon} & = \mathbb{A}_1\epsilon + \mathbb{W}_1\Delta\Phi + \mathbb{B}_1\omega \\ e & = \mathbb{C}_1\epsilon + \mathbb{D}_1\omega. \end{cases} \tag{29}$$

Assuming the Lipschitz condition (4) for $\Phi(x)$, the $\mathcal{H}_\infty$ observer design problem is to determine the matrix Z_1 and Z_2 such that:

- The system (29) is asymptotically stable for $\omega(t) = 0$
- Minimize γ such that $\|e(t)\|_{\mathcal{L}_2} < \gamma\|\omega(t)\|_{\mathcal{L}_2}$ for $\omega(t) \neq 0$

The following theorem solves the above problem into an LMI framework.

Theorem 1. *Consider the system model (3) and the observer (5). The above design problem is solved if there exist a symmetric positive definite matrix X, matrices Y, Z_2 and positive scalar ϵ_l minimizing γ such that:*

$$\begin{bmatrix} \Omega & X\mathbb{W}_1 & XB_{11}+YB_{12} & C_{11}^T+C_{12}^TZ_2^T & C_{11}^T\Gamma_e^T+C_{12}^TZ_2^T\Gamma_e^T \\ \mathbb{W}_1^TX & -\epsilon_l I & 0 & 0 & 0 \\ B_{11}^TX+B_{12}^TY^T & 0 & -\gamma^2 I & D_{11}^T+D_{12}^TZ_2^T & D_{11}^T\Gamma_e^T+D_{12}^TZ_2^T\Gamma_e^T \\ C_{11}+Z_2C_{12} & 0 & D_{11}+Z_2D_{12} & -I & 0 \\ \Gamma_eC_{11}+\Gamma_eZ_2C_{12} & 0 & \Gamma_eD_{11}+\Gamma_eZ_2D_{12} & 0 & -\epsilon_l I \end{bmatrix} < 0 \tag{30}$$

where $\Omega = A_{11}^TX + XA_{11} + A_{12}^TY^T + YA_{12}$,
the matrix Z_1 is then deduced as $Z_1 = X^{-1}Y$.

Proof. Consider the following Lyapunov function candidate

$$V(\cdot) = \epsilon(\cdot)^TX\epsilon(\cdot). \tag{31}$$

Differentiating $V(\cdot)$ along the solution of (29) yields

$$\begin{aligned}\dot{V}(\cdot) = \dot{\epsilon}^TX\epsilon + \epsilon^TX\dot{\epsilon} = \epsilon^T(\mathbb{A}_1^TX + X\mathbb{A}_1)\epsilon + \Delta\Phi^T\mathbb{W}_1(\rho)^TX\epsilon + \omega^T\mathbb{B}_1^TX\epsilon \\ + \epsilon^TX\mathbb{W}_1(\rho)\Delta\Phi + \epsilon^TX\mathbb{B}_1\omega\end{aligned} \tag{32}$$

In order to satisfy the $\mathcal{H}_\infty$ performance objective w.r.t. the $\mathcal{L}_2$ gain disturbance attenuation, we need to consider the following inequality

$$\begin{aligned}&\dot{V} + e^Te - \gamma^2\omega^T\omega < 0 \\ \Leftrightarrow &\begin{bmatrix} \epsilon^T \\ \Delta\Phi^T \\ \omega^T \end{bmatrix}^T \begin{bmatrix} \mathbb{A}_1^TX + X\mathbb{A}_1 + \mathbb{C}_1^T\mathbb{C}_1 & X\mathbb{W}_1 & X\mathbb{B}_1 + \mathbb{C}_1^T\mathbb{D}_1 \\ \mathbb{W}_1^TX & 0 & 0 \\ \mathbb{B}_1^TX + \mathbb{D}_1^T\mathbb{C}_1 & 0 & \mathbb{D}_1^T\mathbb{D}_1 - \gamma^2 I \end{bmatrix} \begin{bmatrix} \epsilon \\ \Delta\Phi \\ \omega \end{bmatrix} < 0\end{aligned} \tag{33}$$

Defining $\eta = \begin{bmatrix} \epsilon \\ \Delta\Phi \\ \omega \end{bmatrix}$, one obtains

$$\eta^TM\eta < 0 \tag{34}$$

where $M = \begin{bmatrix} \mathbb{A}_1^TX + X\mathbb{A}_1 + \mathbb{C}_1^T\mathbb{C}_1 & X\mathbb{W}_1 & X\mathbb{B}_1 + \mathbb{C}_1^T\mathbb{D}_1 \\ \mathbb{W}_1^TX & 0 & 0 \\ \mathbb{B}_1^TX + \mathbb{D}_1^T\mathbb{C}_1 & 0 & \mathbb{D}_1^T\mathbb{D}_1 - \gamma^2 I \end{bmatrix}$

From the Lipschitz condition (4) and u bounded by 1, the following condition is obtained

$$(\Delta\Phi)^T\Delta\Phi \leqslant (\mathbb{C}_1\epsilon + \mathbb{D}_1\omega)^T\Gamma_e^T\Gamma_e(\mathbb{C}_1\epsilon + \mathbb{D}_1\omega) \Leftrightarrow \eta^T Q\eta \leqslant 0 \tag{35}$$

where $Q = \begin{bmatrix} -\mathbb{C}_1^T\Gamma_e^T\Gamma_e\mathbb{C}_1 & 0 & -\mathbb{C}_1^T\Gamma_e^T\Gamma_e\mathbb{D}_1 \\ 0 & I & 0 \\ -\mathbb{D}_1^T\Gamma_e^T\Gamma_e\mathbb{C}_1 & 0 & -\mathbb{D}_1^T\Gamma_e^T\Gamma_e\mathbb{D}_1 \end{bmatrix}$

By applying the $\mathcal{S}$-procedure [2] to the contraint (35) and the condition $\dot{V}(\cdot) + e^Te - \gamma^2\omega^T\omega < 0$ if there exists a scalar $\epsilon_l > 0$ such that

$$\eta^T(M - \epsilon_l Q)\eta < 0 \tag{36}$$

The condition (36) is equivalent to

$$\begin{bmatrix} \Omega_1 + \mathbb{C}_1^T\mathbb{C}_1 + \epsilon_l\mathbb{C}_1^T\Gamma_e^T\Gamma_e\mathbb{C}_1 & X\mathbb{W}_1 & X\mathbb{B}_1 + \mathbb{C}_1^T\mathbb{D}_1 + \epsilon_l\mathbb{C}_1^T\Gamma_e^T\Gamma_e\mathbb{D}_1 \\ \mathbb{W}_1^TX & -\epsilon_l I & 0 \\ \mathbb{B}_1^TX + \mathbb{D}_1^T\mathbb{C}_1 + \epsilon\mathbb{D}_1^T\Gamma_e^T\Gamma_e\mathbb{C}_1 & 0 & \mathbb{D}_1^T\mathbb{D}_1 + \epsilon\mathbb{D}_1^T\Gamma_e^T\Gamma_e\mathbb{D}_1 - \gamma^2 I \end{bmatrix} < 0 \tag{37}$$

where $\Omega_1 = \mathbb{A}_1^TX + X\mathbb{A}_1$

By applying Schur complement to (37), one obtains

$$\begin{bmatrix} \Omega_1 & X\mathbb{W}_1 & X\mathbb{B}_1 & \mathbb{C}_1^T & \mathbb{C}_1^T\Gamma_e^T \\ \mathbb{W}_1^TX & -\epsilon_l I & 0 & 0 & 0 \\ \mathbb{B}_1^TX & 0 & -\gamma^2 I & \mathbb{D}_1^T & \mathbb{D}_1^T\Gamma_e^T \\ \mathbb{C}_1 & 0 & \mathbb{D}_1 & -I & 0 \\ \Gamma_e\mathbb{C}_1 & 0 & \Gamma_e\mathbb{D}_1 & 0 & -\epsilon_l I \end{bmatrix} < 0 \tag{38}$$

Substituting (24)-(28) into (38), the following inequality is obtained

$$\begin{bmatrix} \Omega_2 & X\mathbb{W}_1 & X(B_{11} + Z_1B_{12}) & (C_{11} + Z_2C_{12})^T & (C_{11} + Z_2C_{12})^T\Gamma_e^T \\ \mathbb{W}_1^TX & -\epsilon_l I & 0 & 0 & 0 \\ (B_{11} + Z_1B_{12})^TX & 0 & -\gamma^2 I & (D_{11} + Z_2D_{12})^T & (D_{11} + Z_2D_{12})^T\Gamma_e^T \\ C_{11} + Z_2C_{12} & 0 & D_{11} + Z_2D_{12} & -I & 0 \\ \Gamma_e(C_{11} + Z_2C_{12}) & 0 & \Gamma_e(D_{11} + Z_2D_{12}) & 0 & -\epsilon_l I \end{bmatrix} < 0 \tag{39}$$

where $\Omega_2 = (A_{11} + Z_1A_{12})^TX + X(A_{11} + Z_1A_{12})$.

Let define $Y = XZ_1$ and substitute into (39), the LMI (30) is obtained.

If (30) is satisfied, from (35), (36) implies that

$$\dot{V} + e^Te - \gamma^2\omega^T\omega < 0. \tag{40}$$

Under the zero initial conditions, taking the integration of (40), we obtain

$$\|e(t)\|_{\mathcal{L}_2}^2 < \gamma^2\|\omega(t)\|_{\mathcal{L}_2}^2. \tag{41}$$

The proof of Theorem 1 is completed. □

The H_∞ observer design steps are summarized as the following algorithm:

Input: The system matrices E A, B, C, D
Output: The observer matrices N, J, H, R, S
Step 1: Check the rank condition,

- If $rank\begin{pmatrix} E \\ C \end{pmatrix} = n_x$, continue step 2.
- If $rank\begin{pmatrix} E \\ C \end{pmatrix} < n_x$, stop.

Step 2: Choose the full rank matrix $M \in \mathbb{R}^{n_x \times n_x}$ according to the condition (14), i.e.

$$rank\begin{pmatrix} M \\ C \end{pmatrix} = n_x$$

.

Step 3: Compute matrices K, T, according to the equations (18). Then compute the matrices α_1, α_2, β_1, β_2 as explained in equations (20) and (23).
Step 4: Calculate the matrices A_{11}, A_{12}, B_{11}, B_{12}, $\mathbb{W}_1$, C_{11}, C_{12}, D_{11}, D_{12} according to the equations (24)-(28).
Step 5: Solve the LMI (30) to find the solution X, Y, Z_2 γ, ϵ_l. Then use X and Y to get the matrix Z_1 following Theorem 1.
Step 6: Determine the observer matrices (N, J, H, R, S) by using the matrices Z_1 and Z_2 obtained in steps 5.

4 Synthesis results and frequency domain analysis

In this section, the proposed method is applied to estimate the road profile in the automotive suspension system.

4.1 Synthesis results

In the INOVE testbed available at GIPSA-lab, the applied control signal u (duty cycle of PWM signal) is taken values in the range of $[0, 1]$. By applying the algorithm 1, we obtain the L_2- induced gain $\gamma = 0.967$, $\epsilon_l = 36$ and the observer matrices N, J, H, R, S.

4.2 Frequency domain analysis

The resulting attenuation of the sensor noises on the estimation errors is shown in Figure 1. According to Figure 1, We can see that the proposed method highlights the effectiveness of measurement noise attenuation, which is indicated in the transfer function e_6/ω.

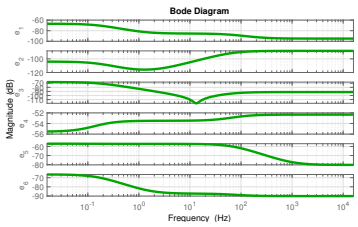

Fig. 1. Transfer $\|e/\omega\|$- Bode diagrams of the proposed observer w.r.t. measurement noise.

5 Simulation result

In this section, three simulations performed with the descriptor system (3) are assessed in the time-domain framework. The initial state conditions for the quarter car system (x_0), the proposed observer (z_0) are chosen as the following:

$$x_0 = \begin{bmatrix}0, 0, 0, 0, 0\end{bmatrix}^T, z_0 = \begin{bmatrix}10\ 0.1\ 0.1\ 10\end{bmatrix}^T$$

In the first scenario, sinusoidal road profile is used. In this simulation, the road profile input is sinusoidal signal with the amplitude at 10^{-3} (m). and the control input u is constant $(u = 0.1)$.

The road estimation results of this scenario are presented in Figures 2. The estimation error is shown at the right side of Figure 2. The NRMSE of this simulation scenario is shown in Table 2. These results highlight the effectiveness of the proposed observer.

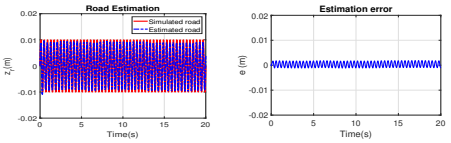

Fig. 2. Scenario 1: (left) Road profile estimation, (right) Estimation error

In the second scenario, ISO road profile is used. In this simulation scenario, the ISO road profile (type C) is used and the control input u is obtained from a Skyhook controller.

The simulation results of the second test is shown in the Fig. 3. To further describe this accuracy, Table 2 presents the normalized root-mean-square errors, considering the difference between the estimated and measured.

In the third scenario, bump road profile is used. In this test, the bump road profile is used and the control input u is constant $(u = 0.1)$.

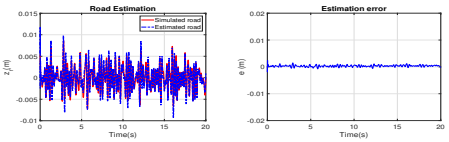

Fig. 3. Scenario 2: (left) Road profile estimation, (right) Estimation error

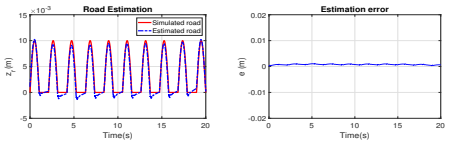

Fig. 4. Scenario 3: (left) Road profile estimation, (right) Estimation error

The estimation results of the third test are shown in Figures 4. According to these figures, we can see that the proposed observer can estimate the bump road precisely.

Table 2. Normalized Root-Mean-Square Errors (NRMSE) of the simulation scenarios

Scenario	Proposed method
Scenario 1	3.97
Scenario 2	1.67
Scenario 3	5.97

6 Conclusions

This paper presented an H_∞ observer to estimate the road profile, using a nonlinear dynamic model of the ER damper. First, the quarter-car system is formulated in a descriptor system which the nonlinearity coming from the damper model is bounded through a Lipschitz condition. The use of two accelerometers, an H_∞ observer, is designed, providing good estimation results of the road profile (not only ISO but also bump road profiles). The estimation error is minimized by using an H_∞ criteria. Simulation results assess the ability proposed method to estimate the road profile of the semi-active damper.

References

1. ASTM: Standard test method for measuring the longitudinal profile of traveled surfaces with an accelerometer established inertial profiling reference (1997)

2. Boyd, S., El Ghaoui, L., Feron, E., Balakrishnan, V.: Linear matrix inequalities in system and control theory, vol. 15. SIAM (1994)
3. Darouach, M., Boutayeb, M.: Design of observers for descriptor systems. IEEE transactions on Automatic Control 40(7), 1323–1327 (1995)
4. Delshad, S.S., Johansson, A., Darouach, M., Gustafsson, T.: Robust state estimation and unknown inputs reconstruction for a class of nonlinear systems: Multiobjective approach. Automatica 64, 1–7 (2016)
5. Doumiati, M., Martinez, J., Sename, O., Dugard, L., Lechner, D.: Road profile estimation using an adaptive youla–kučera parametric observer: Comparison to real profilers. Control Engineering Practice 61, 270–278 (2017)
6. Fialho, I., Balas, G.J.: Road adaptive active suspension design using linear parameter-varying gain-scheduling. IEEE transactions on control systems technology 10(1), 43–54 (2002)
7. Fleps-Dezasse, M., Svaricek, F., Brembeck, J.: Design and experimental assessment of an active fault-tolerant lpv vertical dynamics controller. IEEE Transactions on Control Systems Technology 27(3), 1267–1274 (2019)
8. Ha, Q.P., Trinh, H.: State and input simultaneous estimation for a class of nonlinear systems. Automatica 40(10), 1779–1785 (2004)
9. Healey, A., Nathman, E., Smith, C.: An analytical and experimental study of automobile dynamics with random roadway inputs (1977)
10. Koenig, D., Mammar, S.: Design of proportional-integral observer for unknown input descriptor systems. IEEE transactions on automatic control 47(12), 2057–2062 (2002)
11. Pham, T.P.: LPV observer and Fault-tolerant control of vehicle dynamics: application to an automotive semi-active suspension system. Ph.D. thesis, Université Grenoble Alpes [2020-....] (2020)
12. Pham, T.P., Sename, O., Dugard, L.: Design and experimental validation of an hinf observer for vehicle damper force estimation. IFAC-PapersOnLine 52(5), 673–678 (2019)
13. Pham, T.P., Sename, O., Dugard, L.: Real-time damper force estimation of vehicle electrorheological suspension: A nonlinear parameter varying approach. IFAC-PapersOnLine 52(28), 94–99 (2019)
14. Pham, T.P., Sename, O., Dugard, L.: Unified hinf observer for a class of nonlinear lipschitz systems: Application to a real er automotive suspension. IEEE Control Systems Letters 3(4), 817–822 (2019)
15. Rathai, K.M.M., Sename, O., Alamir, M.: Gpu-based parameterized nmpc scheme for control of half car vehicle with semi-active suspension system. IEEE Control Systems Letters 3(3), 631–636 (2019)
16. Savaresi, S.M., Poussot-Vassal, C., Spelta, C., Sename, O., Dugard, L.: Semi-active suspension control design for vehicles. Elsevier (2010)
17. Solhmirzaei, A., Azadi, S., Kazemi, R.: Road profile estimation using wavelet neural network and 7-dof vehicle dynamic systems. Journal of mechanical science and technology 26(10), 3029–3036 (2012)
18. Stavens, D., Thrun, S.: A self-supervised terrain roughness estimator for off-road autonomous driving. arXiv preprint arXiv:1206.6872 (2012)
19. Tudón-Martínez, J.C., Fergani, S., Sename, O., Martinez, J.J., Morales-Menendez, R., Dugard, L.: Adaptive road profile estimation in semiactive car suspensions. IEEE Transactions on Control Systems Technology 23(6), 2293–2305 (2015)
20. Tudon-Martinez, J.C., Fergani, S., Sename, O., Morales-Menendez, R., Dugard, L.: Online road profile estimation in automotive vehicles. In: 2014 European Control Conference (ECC). pp. 2370–2375. IEEE (2014)